Published in final edited form as:

J Mater Chem B. 2021 June 03; 9(21): 4287–4297. doi:10.1039/d1tb00607j.

Smart Scaffolds: Shape Memory Polymers (SMPs) in Tissue Engineering

Michaela R. Pfau[a], **Melissa A. Grunlan**[*,a,b,c]

[a]Department of Biomedical Engineering, Texas A&M University, College Station, TX 77843, USA.

[b]Department of Materials Science and Engineering, Texas A&M University, College Station, TX 77843, USA.

[c]Department of Chemistry, Texas A&M University, College Station, TX 77843, USA.

Abstract

Smart scaffolds based on shape memory polymer (SMPs) have been increasingly studied in tissue engineering. The unique shape actuating ability of SMP scaffolds has been utilized to improve delivery and/or tissue defect filling. In this regard, these scaffolds may be self-deploying, self-expanding, or self-fitting. Smart scaffolds are generally thermoresponsive or hydroresponsive wherein shape recovery is driven by an increase in temperature or by hydration, respectively. Most smart scaffolds have been directed towards regenerating bone, cartilage, and cardiovascular tissues. A vast variety of smart scaffolds can be prepared with properties targeted for a specific tissue application. This breadth of smart scaffolds stems from the variety of compositions employed as well as the numerous methods used to fabricated scaffolds with the desired morphology. Smart scaffold compositions span across several distinct classes of SMPs, affording further tunability of properties using numerous approaches. Specifically, these SMPs include those based on physically cross-linked and chemically cross-linked networks and include widely studied shape memory polyurethanes (SMPUs). Various additives, ranging from nanoparticles to biologicals, have also been included to impart unique functionality to smart scaffolds. Thus, given their unique functionality and breadth of tunable properties, smart scaffolds have tremendous potential in tissue engineering.

Graphical Abstract

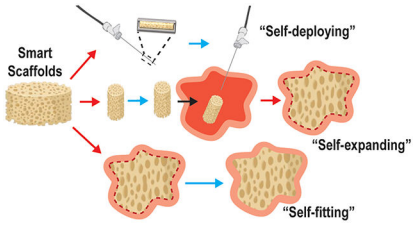

[*]Corresponding Author, mgrunlan@tamu.edu, Tel: +1 979 845 2406.

Author Contributions

The manuscript was written through contributions of all authors. All authors have given approval to the final version of the manuscript.

Conflicts of interest

The authors declare no competing financial interest.

Introduction

Shape memory polymers (SMPs) are a class of smart materials capable of responding to external stimuli with a shape change. This response encompasses shape fixity (deformation followed by fixation into a temporary shape), and shape recovery (a return to the original, permanent shape). “Netpoints” are chemical or physical crosslinks that set the permanent shape whereas “switching segments” allow for fixation into a temporary shape and for recovery back to the permanent shape. Thermoresponsive SMPs, whose shape is modulated by application of heat, have been widely studied. Thermal transition temperatures (T_{trans}) associated with SMP switching segments may either be a glass transition temperature (T_g) or a melting transition temperature (T_m). Thus, a temporary shape formed by deformation at T > T_{trans} can be fixed by cooling to T < T_{trans} and can also be subsequently recovered by heating to T > Ttrans again. For SMPs, the shape memory effect is entropically driven.[1–3]

The unique shape shifting capabilities of SMPs have been used toward advancing numerous biomedical applications.[4–11] In the 1940s, thermoplastic polymer resins with “elastic memory” were developed as dental fillings that could be thermally triggered to expand into tooth cavities.[12] Today, several FDA-approved SMP devices exist, including DYNACORD™ (a self-tightening suture),[13] Eclipse™ (a soft tissue anchor),[14] and Morphix® (an orthopedic suture anchor).[15] More recently, IMPEDE-FX, based on a shape memory polyurethane (SMPU) foam, was approved as an embolization plug. Crimped for catheter delivery, the foam plug undergoes shape recovery (i.e. expansion) within the vasculature as it is hydrated and warmed to body temperature.[16, 17] Bioresorbable SMPs have also been explored extensively, beginning with efforts to develop self-tightening sutures.[4] However, the interest in tissue engineering (TE) has prompted the exploration of biodegradable SMPs as smart scaffolds.[7, 18] Scaffolds play a critical role to regenerate healthy tissues lost to injury, disease, or congenital defects (Figure 1). Exogenous growth factors and/or pre-seeded cells are frequently incorporated into the scaffold to better promote neotissue formation. Scaffold chemical and physical properties have also been shown to potently direct cellular regeneration. Additionally, scaffolds with tailored mechanical properties and degradation profiles are sought to afford the necessary mechanical support and to match the rate of neotissue formation, respectively.[19–21] As smart scaffolds, SMPs offer unique and differentiating characteristics. Namely, this is related to their shape shifting ability, allowing them to fill tissue defects of varying and sometimes irregular geometries with fidelity. Most typically, the shape change is triggered by heat (“thermoresponsive”). Electrically conductive and magnetic scaffolds permit thermally-induced shape actuation via resistive heating and application of a magnetic field, respectively.[22, 23] Some SMP scaffolds that have appreciable hydrophilicity and water-absorbing abilities (e.g. hydrogels) undergo shape change in the form of swelling upon hydration (“hydroresponsive”).[24] In some cases, the absorption of water acts as a plasticizer to reduce the scaffold’s T_{trans} (T_g), resulting in shape recovery.[25, 26] Herein, we highlight recent advances in the use of smart scaffolds with translational potential in TE.

Smart scaffold functionality

Smart SMP scaffolds may be classified according to the nature of functional delivery into tissue defects afforded by shape memory behavior, including self-deploying, self-expanding, and/or self-fitting (Figure 2). These scaffolds leverage their shape fixity and recovery for their minimally invasive delivery, triggered volumetric filling, and/or conformal fitting within irregularly shaped spaces. SMP scaffolds afford the opportunity to achieve excellent contact with adjacent tissue, an integral aspect of tissue integration and healing. Filling of irregular spaces is a feature usually associated with *in situ* forming materials (e.g. bone cements, injectable hydrogels, etc.). However, these are associated with various limitations including exothermic cures, slow setting times, low pore interconnectivity, and shrinkage resulting in loss of contact with adjacent tissues.[27–34] In some cases, the permanent shape and size of the SMP scaffolds is designed to match that of the tissue defect. Alternatively, the SMP scaffold is of a generic geometry but is used to fill various and even irregularly shaped defects.

Self-deploying scaffolds.

Smart SMP scaffolds that self-deploy are typically warmed to their T_{trans} to permit crimping into a compact geometry and subsequently cooled to fix this shape, affording loading into a catheter or needle. Thus, these shape fixed scaffolds can be delivered in a minimally invasive fashion. Self-deploying scaffolds typically have a T_{trans} near body temperature (T_{body} ~37 °C), such that upon delivery, the scaffold is triggered to shape recover (i.e. expand). Hydration that occurs after delivery can also trigger shape recovery.

Self-expanding scaffolds.

While not delivered via minimally invasive techniques, self-expanding scaffolds also undergo shape recovery in tissue defects or voids. The scaffold, previously fixed in a relatively compressed shape, is triggered to expand within the tissue space via shape recovery. Likewise, shape recovery can be initiated by warming to T_{body} and/or hydration upon implantation.

Self-fitting scaffolds.

Self-fitting scaffolds are often based on SMPs having a T_{trans} slightly above T_{body}. These may be warmed (e.g. with saline; $T > T_{trans}$) to cause softening, allowing the scaffold to be press-fitted into the tissue defect. Shape recovery then drives expansion of the scaffold within the defect, including those with irregular geometries. As the scaffold cools to T_{body} ~37 °C, it becomes shape fixed in this new geometry. If cooling occurs too rapidly to permit expansion to defect edges, irrigation with warm saline, if at an acceptably tissue-safe temperature, could be used to promote continued shape recovery. Hydration can also drive self-fitting of a SMP scaffolds into a defect, pending non-brittle mechanical properties permit press-fitting.

Smart scaffolds for targeted tissue regeneration

The advantages associated with delivery, conformal fitting, and/or integration with surrounding host tissue make smart scaffolds excellent candidates for engineering a large variety of tissues (Figure 3 and Table 1). Most particularly, smart scaffolds have been evaluated for bone, cartilage, and cardiovascular tissue regeneration. Herein, we primarily highlight smart scaffolds that have been shown to support the differentiation and proliferation of human mesenchymal stem cell (hMSCs) and/or have advanced to *in vivo* studies.

Bone tissues.

Several smart scaffolds have been developed for bone TE. SMPU scaffolds containing PCL and poly(L-lactic acid) (PLLA) soft segments were blended with poly(ethylene glycol) (PEG) or gelatin to adjust viscosity for fused deposition modeling (FDM) fabrication. Due to water uptake by the PEG or gelatin, the T_{trans} ($T_{g,\ PLLA}$ ~50 °C) was lowered via plasticization to T_{body}, affording a self-expanding scaffold. These scaffolds supported osteogenesis of hMSCs, which was further enhanced via incorporation of superparamagnetic iron oxide (SPIO) nanoparticles (NPs).[35] Another SMPU, prepared using 6-arm star PLLA with an aniline trimer incorporated for electroactivity, showed improved osteogenic differentiation of myoblasts versus those prepared without aniline.[36] SMP films based on UV-curable PCL-dimethacrylate (MA) (PCL-MA) ($T_{trans} = T_{m,\ PCL}$ ~54 °C) supported hMSC differentiation into osteoblasts, even following thermally-triggered shape recovery.[37] Using solvent casting particulate leaching (SCPL), PCL-based scaffolds were prepared with diol-terminated PCL, dextran, and a carbodiimide linker, and then coated with bioactive hydroxyapatite (HAp) via solution precipitation. By adjusting the PCL/dextran ratio, the T_{trans} ($T_{m,\ PCL/dextran}$) was adjusted to ~ T_{body} to support self-expansion, and the scaffolds were shown to support bone MSC (BMSC) osteogenesis. *In vivo* degradation was also monitored in a rat subcutaneous model, and scaffolds were shown to degrade fully within ~6 months.[38]

Other bone TE smart scaffolds have been developed for more targeted scenarios. We have reported self-fitting scaffolds for treatment of irregularly-shaped craniomaxillofacial (CMF) bone defects. PCL-diacrylate (PCL-DA) scaffolds ($T_{trans} = T_{m,\ PCL}$ ~55 °C) were prepared via SCPL with a fused salt template for pore interconnectivity, and subsequently coated with a bioactive polydopamine coating.[39] Scaffolds exhibited HAp mineralization *in vitro*, and, when modified with a cell adhesive peptide, were shown to support osteogenic hMSC differentiation.[40] Intended to treat femoral segmental bone defects, self-expanding scaffolds were prepared from acrylate monomers and a crosslinker (tetraethylene glycol dimethacrylate, tEG-DMA) using SCPL. The ratio of tert-butyl acrylate (tBA) and butyl acrylate (BA) (92:8 wt%) was tuned to achieve a T_{trans} ~ T_{body}. These scaffolds were fixed into a compressed shape, and subsequent irrigation with 45 °C saline triggered scaffold expansion into a mouse femoral defect. Overall, these SMP grafts showed integration with native bone after 12 weeks, and torsional mechanical properties comparable to an allograft.[41] To treat a confined femoral bone defect, a PCL-HAp SMP scaffold ($T_{trans} = T_{m,\ PCL}$ ~40 °C) was prepared via gas foaming. A shape fixed, compressed scaffold was implanted into a

rabbit femoral defect, where irrigation with warm saline prompted self-expansion. After 12 weeks, bone ingrowth at the periphery and neovascularization was observed.[42]

Cartilage tissues.

Several smart scaffolds have been designed to repair cartilage, including the various types found in joints, ears, intervertebral discs, and trachea. Many of these are hydrogels and so are hydroresponsive. Targeted for articular cartilage repair, a self-expanding alginate gel, cross-linked via carbodiimide chemistry, was prepared with aligned pores via directional freezing. These scaffolds exhibited robust mechanical properties and were capable of reversible compression. Aligned pores allowed for improved collagen deposition by cultured hMSCs and was further improved with a Type II collagen coating.[43] Another self-expanding hydrogel scaffold, prepared with collagen or denatured collagen and a carbodiimide cross-linker, was used to treat full thickness defects in the knee joints of NZ white rabbits. These smart scaffolds, optionally pre-seeded with chondrocytes, promoted cartilage and subchondral bone repair.[44] Smart scaffolds were prepared via SCPL using poly(glycerol sebacate) (PGS) and poly(1,3-propylene sebacate) (PPS) as well as bioactive kartogenin (KGN). These acellular scaffolds could be prepared with a broad T_{trans} ($T_{m,\ PGS}$ ~35–45 °C), and so exhibited excellent shape recovery at T_{body} as well as supported chondrogenic differentiation of BMSCs. Furthermore, acellular scaffolds were self-deployed into full-thickness defects of the rat femoropatellar groove where they supported chrondrogenic differentiation and formation of neocartilage.[45] A smart scaffold was developed to mimic the complexly shaped auricular cartilage of human ears. PLLA threads were woven into mesh tubes that, upon heating above the T_{trans} ($T_{g,\ PLLA}$ ~60 °C), could be molded into helical shapes like those of human ears. These scaffolds were seeded with cartilaginous particles derived from human pluripotent stem (iPS) cells and implanted subcutaneously into a mouse model where the shape and cartilage features were maintained for one year.[46] For tracheal repair, a smart scaffold was prepared from a PLLA iron-oxide (Fe_3O_4) nanocomposite ($T_{trans} = T_{g,\ PLLA}$ ~ 65 °C) using FDM. The Fe_3O_4 NPs were shown to permit magnetically-induced thermal actuation when exposed to a 30 kHz alternating magnetic field.[47] Targeted for the repair of annulus fibrosus (AF) tissue in herniated intervertebral discs, a hydroresponsive, alginate/carbodiimide-linked self-expanding hydrogel scaffold was evaluated. These were shown to support AF cell proliferation and adhesion with extracellular matrix (ECM) secretion after 21 days in culture with transforming growth factor beta 3 (TGF-β3) supplementation.[48]

Cardiovascular tissues.

Smart scaffolds have been frequently directed towards cardiovascular TE, including in the form of cardiac patches, vascular grafts, and vascular wraps. Smart cardiac patches were prepared from a soybean oil epoxidized acrylate network as thin film with complex porous micropatterns using stereolithography. These patches were designed to be self-expanding ($T_{trans} \sim T_{body}$) and were shown to support hMSC cardiomyogenic differentiation.[49] To permit minimally invasive delivery, a smart scaffold was prepared as an injectable cardiac patch from elastic poly(octamethylene maleate (anhydride) citrate)) microfabricated with a diamond-shaped lattice which drives shape recovery. These smart patches were seeded with rat cardiomyocytes (CMs) and were self-deployed (i.e. injected) into a myocardial infarction

rat model where they were shown to increase wall thickness. The same type of cardiac patches, but seeded with human stem cell derived CMs and scaled up in size, were also successfully delivered via minimally invasive surgical techniques into a porcine model.[50]

Smart scaffolds have also been utilized to prepare vascular grafts. A 6-armed poly(ethylene glycol)-PCL-acrylate (PEG-PCL-Ac) was melt casted and UV-cured over a mold to afford micropatterned pores of different geometries on each side. To permit minimally invasive delivery, the scaffold (T_{trans} ~ T_{body}) was shape fixed into a tightly rolled conformation and expansion (i.e. shape recovery) triggered by body temperature. These were successfully implanted into the cervical artery of NZ white rabbits and supported endothelial cells (ECs) on the surface with vascular smooth muscle cells (VSMCs) on the inner surface.[51] A smart vascular scaffold based on 4D-printed biodegradable poly(glycerol dodecanoate)-Ac (PGD-Ac) exhibited a tunable T_{trans} (20–37 °C), depending on the duration of thermal curing. In this way, the scaffold was successfully implanted as a self-expanding vascular graft into a mouse aorta and supported endothelial and smooth muscle cell proliferation.[52] A perivascular smart wrap based on PCL-*co*-(α-allyl carboxylate ε-caprolactone) (PCL-*co*-ACPCL) was UV-cured into a film and then porated via laser ablation. Following implantation into mouse subcutaneous tissue, the microporous scaffolds showed upregulated neovascularization, fibrogenesis, and angiogenesis. Having a T_{trans} ~ T_{body}, these scaffolds are expected to actuate upon implantation to afford self-wrapping.[53]

Other tissues.—For skeletal muscle, a freeze-dried alginate/carbodiimide-linked self-deploying hydroresponsive scaffold was delivered via minimally invasive techniques in a severe skeletal muscle mouse injury model. The dehydrated scaffold was loaded into a needle and the syringe then filled with myoblasts and growth factors (e.g. insulin-like growth factor 1 (IGF-1) and vascular endothelial growth factor (VEGF)) to improve cell engraftment and muscle contraction.[54] To treat neuronal tissue damage caused by severe ischemic stroke, hydroresponsive scaffolds based on carbon nanotube (CNT)-doped silkworm sericin were prepared with geometries to match that of an irregularly-shaped cavity in an ischemic stroke mouse model. Following pre-seeding with BMSCs, these scaffolds were delivered via minimally invasive procedures and were shown to support neuronal differentiation.[55]

SMP materials, scaffold fabrication, and property tunability

As evidenced by the many smart scaffolds evaluated for various TE applications, a variety of SMP materials have been utilized (Figure 4). All SMPs must include two functional design elements: netpoints (responsible for the memorized shape or “shape recovery”) and switching segments (responsible for the temporary programmed shape or “shape fixity”). These elements can be achieved via differing network designs, including physically cross-linked, chemically cross-linked, or PUs, which may rely on physical and/or chemical cross-linking. Variations of each of these affords additional tunability of shape memory behavior, and important material properties (e.g. modulus, and degradation rate). Moreover, fabrication methods can be used to further enhance SMP scaffold efficacy.

Physically cross-linked.

As noted above, two examples of PLLA-based physically cross-linked smart scaffolds were developed toward the regeneration of ear cartilage and tracheal tissue. For thermoplastic PLLA, where crystalline lamellae serve as netpoints and amorphous chain segments act as switching segments. Typically, T_g of PLLA (T_g ~ 50–65 °C, depending on molecular weight)[56] serves as the T_{trans}, and so body temperature cannot trigger shape recovery. However, this T_{trans} range is ideal for maintaining a fixed shape upon implantation, as for Uto's ear regeneration study.[46] Alternatively, incorporating magnetic nanoparticles, as in the tracheal scaffold study, can provide remote shape actuation of PLLA-based smart scaffolds.[47]

Physically cross-linked SMPs may be refined via copolymerization, formation of nanocomposites, and by blending. Poly(D,L-lactide)-*co*-trimethylene carbonate (PDLLA-TMC) and poly(lactide-glycolide)-TMC (PLGA-TMC) copolymers were electrospun into scaffolds for bone and vascular TE, respectively. The TMC was used to tune the T_g to ~ T_{body} and physical cross-links were afforded by chain entanglements.[57, 58] Likewise, biodegradable amorphous poly(propylene carbonate) (PPC) exhibits shape memory (T_{trans} ~ T_g ~ 60 °C) that was shown to be enhanced following the addition of microfibrillated cellulose as a composite.[59] PLA-based composites have also been prepared with chitosan for potential antimicrobial activity[60] as well as with graphene for electrical SMP activation.[61] Blending PLA with PCL has been commonly used as a strategy to improve PLA toughness, and depending on the PLA/PCL weight percent, has also been shown to exhibit shape memory with PCL crystalline lamellae as the switching segment (T_{trans} ~ $T_{m,PCL}$ ~55 °C).[62] PLA/PCL blends have also been combined with nanohydroxyapatite (nHA) as bioactive nanocomposites.[63] Physically immiscible blends, like the PLA/PCL constructs, attain shape memory behavior due to phase separation, which allows one phase (PLA) to behave as the netpoints, while the other phase (PCL) behaves as the switching segment. PLLA has also been blended, but in a miscible system, with poly(3-hydroxybutarate-co-hydroxyvalerate) (PHBV) to lower T_{trans} toward T_{body} and PLLA/PHBV blends prepared as scaffolds via electrospinning were shown to support osteogenesis of BMSCs.[64, 65] Miscible PLLA/poly(methyl-methacrylate) (PMMA) blends have been shown to have a broad T_g that allows for triple shape memory.[66] PLLA/poly(vinyl acetate) (PVAc) blends were also shown to be miscible but the incorporation of nanohydroxyapatite (nHA) or graphene can lead to phase separation and induce triple shape memory via two distinct thermal transitions.[61, 67] The addition of nHA may also be advantageous to bone TE in providing an osteoconductive environment for mineralization, while nanocarbons like graphene may allow for electrical trigger of shape memory via resistive heating.

Chemically cross-linked.

Various chemically cross-linked SMPs have been used to prepare smart scaffolds for TE, as noted above. In these systems, chemical cross-links act as netpoints while polymer segments between cross-links act as switching segment. Like physically cross-linked systems, shape memory can be actuated thermally and/or via hydration but chemically cross-linked systems tend to have more robust shape recovery. Acrylate (Ac)- or methacrylate (MA)-based networks, prepared from macromers with these terminal crosslinkable groups, have been

commonly used toward both bone and cardiovascular TE.[37, 39, 40, 49, 53] These form networks comprised of crosslinks (i.e. netpoints) consisting of hydrolysable esters. Semi-crystalline PCL has been particularly utilized, since the T_m (~43–60°C) generally decreases with decreased molecular weight (M_n), the T_{trans} (T_m) may be tuned.[68] Additional modifications to PCL-network scaffolds can afford properties useful to regeneration. For instance, we have made numerous modifications to smart scaffolds for CMF defects formed from PCL networks using SCPL fabrication.[39, 69] To impart bioactivity, a polydopamine coating was applied to PCL-DA scaffolds.[40] In another approach, SMP scaffolds were likewise prepared as co-networks with macromers comprised of PCL and polydimethylsiloxane (PDMS) segments.[70] Attributed to the silicon-based and hydrophobic nature of the PDMS, these PCL-PDMS scaffolds exhibited HAp mineralization *in vitro*. Using a semi-interpenetrating network (semi-IPN) design based on PCL-DA and thermoplastic PLLA scaffolds were also prepared with accelerated degradation and increased modulus.[71] Lastly, using a star-PCL architecture, we showed that the T_{trans} could be reduced to ~45 °C ($T_{m,PCL}$) for improved tissue safety during thermally driven self-fitting. Cardiovascular TE scaffolds based on PGD-Ac networks represent another type of acrylate network with PGD switching segments having a T_{trans} ($T_{g,\ PGD}$) that can be readily tuned to ~T_{body} via cure time.[72] Acrylate-based networks have also been used to form other chemically crosslinked SMP scaffolds. These include bone TE scaffolds based on butyl-based monomers as well as soybean epoxidize acrylate. As noted above, the T_{trans} (T_g) can be tuned to ~ T_{body} with monomer ratio[41] and could also be formed with acrylated PEG to afford plasticization (i.e. T_g lowering) due to hydration.[73] Similarly, methacrylate (MA) macromers were used to form PCL/PEG (“CLEG”) co-network hydrogels with shape memory properties.[74] PTMC-MA macromers have also been used to form chemically cross-linked SMPs, and have been combined as nanocomposites with PLA fibers,[75] plasticized with PEG co-networks, and copolymerized with PDLLA to tune properties.[76] Chemical cross-linking moieties based on radical crosslinking can also be introduced into polymer repeat unit pendant groups or backbone. For instance, PCL-based copolymer having crosslinkable pendant allyl groups were used to prepare SMP scaffolds for vascular TE and whose T_{trans} (T_m) could be adjusted to ~ T_{body} based on the ratio of ε-caprolactone (CL) to α-allyl carboxylate-CL.[53, 77] Co-polyesters containing fumaric acid (FA) segments, bearing crosslinkable double bonds in the backbone, have been prepared as hydroresponsive scaffolds via SCPL.[78] SMP scaffolds for bone TE were recently prepared by 4D printing of poly(propylene fumarate) (PPF). These PFF scaffolds exhibited a tunable T_{trans} (T_g ~30–40 °C) depending on cure time.[79]

Chemically cross-linked networks have been prepared with other cross-linking chemistries as well. Examples include, PTMC cross-linked with a bis(cyclic carbonate) via ring opening polymerization (ROP),[80] PCL/PEG co-networks cross-linked via thiol-ene chemistry,[81] and alginate or collagen hydrogels cross-linked with via carbodiimide chemistry.[43, 44, 48, 54, 82, 83] Several other carbodiimide cross-linked hydrogel scaffolds were described earlier, often prepared via freeze-drying or lyophilization.[43, 48, 54] Smart hydrogel scaffolds have also been prepared as interpenetrating networks (IPN) cryogels consisting of covalently and permanently crosslinked polyacrylamide (PAAm) and covalently and dynamically

crosslinked oligoethylene glycol (OEG)-based dendronized polymers. The Schiff-base cross-linking allow for dynamic, pH-modulated control over shape memory.[84]

Polyurethanes.

SMPUs are a distinct class of widely studies SMPs, relying on physical cross-linking (thermoplastics) or chemical cross-linking (thermosets). SMPUs are generally characterized by thermodynamically immiscible soft segments (switching segments) and hard segments (netpoints). These are connected via urethane linkages formed through reactions of alcohol and isocyanate moieties. Chain extenders, low molecular weight diols (or diamines), may be reacted with diisocyanates to increase the length of the hard segments.[85] Thermoplastic PUs (TPUs) are formed into physically cross-linked PU scaffolds frequently via electrospinning or 3D-printing, where the molecular weight of these types of chains yields conducive rheological properties. TPUs have been modified in many common ways that have been previously described for other SMP systems, including: PCL-based co-polymers,[86, 87] PLA-based blends,[88, 89] bio-based (i.e. castor oil) precursors,[7] combining with hydrophilic polymers,[35] and nanocomposites.[88] CNT,[90] HAp,[91] and iron-based NPs seen in previous systems have been employed in TPUs. One nanocomposite SMP not previously discussed is a PLA-based TPU with nanosilicates, shown to induce HAp mineralization for bone TE.[92]

Chemically cross-linked SMPU porous scaffolds are frequently formed via gas foaming. In this process, pre-polymers with isocyanate moieties react with polyols to produce PU linkages, and carbon dioxide (CO_2) generation occurs as a by-product of the reaction between excess isocyanates and water. This process also usually employs a combination of catalysts, surfactants, heat, and blowing agents.[93, 94] Maitland et al. utilized gas foaming to create smart SMPU embolization devices,[25, 95, 96] including those that are modified with tungsten NPs for radio-opacity.[97] Other chemically cross-linked SMPUs have used NPs that are functionalized to act as chemical cross-linkers. For instance, oxidized CNTs[98] and star-shaped polyester having a polyhedral oligomeric silsesquioxane (POSS)core[99] have been employed as multifunctional cross-linkers. Polymers typically used to construct smart scaffolds and methods to achieve tunability of properties are summarized in Figure 5. In addition to thermoresponsive and hydroresponsive SMP scaffolds, another class of SMPs are elastomers that can be fabricated into mesh lattices (typically via 3D printing) whose geometries support SMP abilities, as previously noted for the cardiac patch example.[50, 100] To participate in cell-like signaling, other SMP scaffolds may leverage dynamic linkages, including those based on Schiff bases[18] and ionic chemistries. One major class of these are chitosan-based SMP systems as chitosan can crosslink via link via physical, chemical, or ionic linkages.[101, 102] The ionic linkages have the potential to be controlled by pH,[103] and so could be utilized to produce shape memory behavior.

Conclusions

Smart scaffolds based on thermoresponsive and hydroresponsive SMPs hold vast potential to advance the regeneration of numerous tissues, particularly bone, cartilage, and cardiovascular tissues. The shape memory ability of smart scaffolds has largely been leveraged to achieve tissue defect filling, either via self-deploying, self-expanding, or self-

fitting. This unique feature affords convenient routes for implantation as well as superior scaffold-tissue contact to promote healing. Collectively, SMP scaffolds possess a breadth of useful properties that afford further tunability through a variety of strategies. SMP materials used to prepare scaffolds can be classified as physically cross-linked, chemically cross-linked, or SMPUs. Within each of these classes of SMPs, a variety of fabrication methods can be used to prepare smart scaffolds with specific morphological features. More recently, the shape shifting ability of SMPs has been utilized to respond to cellular triggers[104] or for on/off switching of cell behavior (e.g. alignment and differentiation).[105–107] Such SMPs have the potential to create smart scaffolds with greater control over directing tissue regeneration.

Increasing evidence of the utility of smart scaffolds is supported by a growing body of work with cultured stem cells as well as with animal models. However, a remaining challenge is clinical translation, evident in the lack of smart scaffolds currently available on the market. The first SMP device to receive FDA approval as a permanent implant was the WedgeLoc suture anchor, now referred to as Morphix®, as noted herein in the Introduction.[15, 108] Also noted in the Introduction, the Impede-FX SMP device recently gained FDA 510 (k) clearance in 2019 as an embolization plug. Significantly, this is the first porous and biodegradable SMP device to achieve such clearance.[16, 17] A regulatory hurdle to consider is that 510 (k) clearance relies on comparisons to a “substantially equivalent” approved device. This may make the pathway to approval more feasible for smart scaffolds that can act as substitutes for existing devices such as bone void fillers.[109] Moreover, the incorporation of functional additives, and/or pre-seeded cells may present further regulatory hurdles as they convolute device classification. But the FDA recently released a new guidance on evaluation of regenerative devices to “simplify and streamline” approval of such combinatory therapies.[110] Thus, the development of smart scaffolds is making promising headway towards clinical translation in regenerative engineering.

Acknowledgements

Funding from NIH NIDCR 1R01DE025886-01A1 and the Texas A&M Engineering Experiment Station is gratefully acknowledged.

References

1. Behl M and Lendlein A, Mater. Today Commun, 2007, 10, 20–28.
2. Behl M and Lendlein A, Soft Matter, 2007, 3, 58–67.
3. Lendlein A, J. Mater. Chem, 2010, 20, 3332–3334.
4. Lendlein A and Langer R, Science, 2002, 296, 1673. [PubMed: 11976407]
5. Delaey J, Dubruel P and Van Vlierberghe S, Adv. Funct. Mater, 2020, 30, 1909047.
6. Lendlein A, Behl M, Hiebl B and Wischke C, Expert Rev. Med. Devices, 2010, 7, 357–379. [PubMed: 20420558]
7. Hasan SM, Nash LD and Maitland DJ, J. Polym. Sci., Part B: Polym. Phys, 2016, 54, 1300–1318.
8. Small IVW, Singhal P, Wilson TS and Maitland DJ, J. Mater. Chem, 2010, 20, 3356–3366. [PubMed: 21258605]
9. Yakacki CM and Gall K, in Shape-Memory Polymers, ed. Lendlein A, Springer Berlin Heidelberg, Berlin, Heidelberg, 2010, pp. 147–175.
10. Wang K, Strandman S and Zhu XX, Front. Chem. Sci. Eng, 2017, 11, 143–153.

11. Chen H-M, Wang L and Zhou S-B, Chin. J. Polym. Sci, 2018, 36, 905–917.
12. Vernon L and Vernon H, US patent, 1941, 2234993.
13. Metz RM and Kaar SG, Oper. Tech. Orthop, 2020, 30, 100818.
14. Christensen J, Fischer B, Nute M and Rizza R, J. Foot Ankle Surg, 2018, 57, 60–64. [PubMed: 29268903]
15. Berg-Johansen B, Lovald S, Altiok E and Kurtz SM, in PEEK Biomaterials Handbook (Second Edition), ed. Kurtz SM, William Andrew Publishing, 2019, pp. 291–300.
16. Morgan RA, Loftus I, Ratnam L, Das R, Mailli L, Hamady M and Lobotesis K, CVIR Endovasc, 2021, 4, 1–9. [PubMed: 33387046]
17. Jansen A-JS, van Schaik PM, Martens JM and Reijnen MM, CVIR Endovasc, 2020, 3, 1–5. [PubMed: 32027004]
18. Zhang K, Wang S, Zhou C, Cheng L, Gao X, Xie X, Sun J, Wang H, Weir MD, Reynolds MA, Zhang N, Bai Y and Xu HHK, Bone Res, 2018, 6, 31. [PubMed: 30374416]
19. Dhandayuthapani B, Yoshida Y, Maekawa T and Kumar DS, Int. J. Polym. Sci, 2011, 2011, 290602.
20. Qu H, Fu H, Han Z and Sun Y, RSC Adv, 2019, 9, 26252–26262.
21. Hollister SJ, Nat. Mater, 2005, 4, 518–524. [PubMed: 16003400]
22. Leng J, Lan X, Liu Y and Du S, Prog. Mater. Sci, 2011, 56, 1077–1135.
23. Liu Y, Lv H, Lan X, Leng J and Du S, Compos. Sci. Technol, 2009, 69, 2064–2068.
24. Shang J, Le X, Zhang J, Chen T and Theato P, Polym. Chem, 2019, 10, 1036–1055.
25. Jang LK, Fletcher GK, Monroe MBB and Maitland DJ, J. Biomed. Mater. Res. A, 2020, 108, 1281–1294. [PubMed: 32061006]
26. Cai S, Sun Y-C, Ren J and Naguib HE, J. Mater. Chem. B, 2017, 5, 8845–8853. [PubMed: 32264278]
27. Lennon AB and Prendergast PJ, J. Biomech, 2002, 35, 311–321. [PubMed: 11858806]
28. Lobb DC, DeGeorge BR and Chhabra AB, J. Hand Surg, 2019, 44, 497–505.e492.
29. Orr JF, Dunne NJ and Quinn JC, Biomaterials, 2003, 24, 2933–2940. [PubMed: 12742733]
30. Hou Q, De Bank PA and Shakesheff KM, J. Mater. Chem, 2004, 14, 1915–1923.
31. Migliaresi C, Motta A and DiBenedetto AT, in Engineering of Functional Skeletal Tissues, eds. Bronner F, Farach-Carson MC and Mikos AG, Springer London, London, 2007, pp. 95–109.
32. Van der Stok J, Van Lieshout EM, El-Massoudi Y, Van Kralingen GH and Patka P, Acta Biomater, 2011, 7, 739–750. [PubMed: 20688196]
33. Low KL, Tan SH, Zein SH, Roether JA, Mouriño V and Boccaccini AR, J. Biomed. Mater. Res. B Appl. Biomater, 2010, 94, 273–286. [PubMed: 20336722]
34. Serbetci K, Korkusuz F and Hasirci N, Polym. Test, 2004, 23, 145–155.
35. Wang Y-J, Jeng US and Hsu S.-h., ACS Biomater. Sci. Eng, 2018, 4, 1397–1406. [PubMed: 33418669]
36. Xie M, Wang L, Ge J, Guo B and Ma PX, ACS Appl. Mater. Interfaces, 2015, 7, 6772–6781. [PubMed: 25742188]
37. Neuss S, Blomenkamp I, Stainforth R, Boltersdorf D, Jansen M, Butz N, Perez-Bouza A and Knüchel R, Biomaterials, 2009, 30, 1697–1705. [PubMed: 19121539]
38. Huang K, Yang M.-s., Tang Y.-j., Ling S-Y, Pan F, Liu X.-d. and Chen J, J. Biomater. Appl, 2020, 35, 823–837. [PubMed: 32842853]
39. Zhang D, George OJ, Petersen KM, Jimenez-Vergara AC, Hahn MS and Grunlan MA, Acta Biomater, 2014, 10, 4597–4605. [PubMed: 25063999]
40. Erndt-Marino JD, Munoz-Pinto DJ, Samavedi S, Jimenez-Vergara AC, Diaz-Rodriguez P, Woodard L, Zhang D, Grunlan MA and Hahn MS, ACS Biomater. Sci. Eng, 2015, 1, 1220–1230. [PubMed: 33304994]
41. Baker RM, Tseng L-F, Iannolo MT, Oest ME and Henderson JH, Biomaterials, 2016, 76, 388–398. [PubMed: 26561935]
42. Xie R, Hu J, Hoffmann O, Zhang Y, Ng F, Qin T and Guo X, Biochim. Biophys. Acta, 2018, 1862, 936–945.

43. Almeida HV, Sathy BN, Dudurych I, Buckley CT, O'Brien FJ and Kelly DJ, Tissue Eng. Part A, 2016, 23, 55–68. [PubMed: 27712409]
44. Jiang LB, Su DH, Liu P, Ma YQ, Shao ZZ and Dong J, Osteoarthr. Cartil, 2018, 26, 1389–1399.
45. Xuan H, Hu H, Geng C, Song J, Shen Y, Lei D, Guan Q, Zhao S and You Z, Acta Biomater, 2020, 105, 97–110. [PubMed: 31953195]
46. Uto S, Hikita A, Sakamoto T, Mori D, Yano F, Ohba S, Saito T, Takato T and Hoshi K, Tissue Eng. Part A, 2020.
47. Zhao W, Zhang F, Leng J and Liu Y, Compos. Sci. Technol, 2019, 184, 107866.
48. Guillaume O, Daly A, Lennon K, Gansau J, Buckley SF and Buckley CT, Acta Biomater, 2014, 10, 1985–1995. [PubMed: 24380722]
49. Miao S, Zhu W, Castro NJ, Nowicki M, Zhou X, Cui H, Fisher JP and Zhang LG, Sci. Rep, 2016, 6, 27226. [PubMed: 27251982]
50. Montgomery M, Ahadian S, Davenport Huyer L, Lo Rito M, Civitarese RA, Vanderlaan RD, Wu J, Reis LA, Momen A, Akbari S, Pahnke A, Li R-K, Caldarone CA and Radisic M, Nat. Mater, 2017, 16, 1038–1046. [PubMed: 28805824]
51. Liu D, Xiang T, Gong T, Tian T, Liu X and Zhou S, ACS Appl. Mater. Interfaces, 2017, 9, 19725–19735. [PubMed: 28540725]
52. Zhang C, Cai D, Liao P, Su J-W, Deng H, Vardhanabhuti B, Ulery BD, Chen S-Y and Lin J, Acta Biomater, 2021, 122, 101–110. [PubMed: 33359298]
53. Boire TC, Himmel LE, Yu F, Guth CM, Dollinger BR, Werfel TA, Balikov DA and Duvall CL, J. Biomed. Mater. Res. A, 2021, 109, 272–288. [PubMed: 32490564]
54. Wang L, Cao L, Shansky J, Wang Z, Mooney D and Vandenburgh H, Mol. Ther, 2014, 22, 1441–1449. [PubMed: 24769909]
55. Wang J, Li X, Song Y, Su Q, Xiaohalati X, Yang W, Xu L, Cai B, Wang G, Wang Z and Wang L, Bioact. Mater, 2021, 6, 1988–1999. [PubMed: 33474513]
56. Ahmed J and Varshney SK, Int. J. Food Prop, 2011, 14, 37–58.
57. Bao M, Lou X, Zhou Q, Dong W, Yuan H and Zhang Y, ACS Appl. Mater. Interfaces, 2014, 6, 2611–2621. [PubMed: 24476093]
58. Chen M, Li L, Xia L, Zhang F, Jiang S, Hu H, Li X and Wang H, Macromol. Biosci, 2020, 20, 1900312.
59. Qi X, Yang G, Jing M, Fu Q and Chiu F-C, Journal of Materials Chemistry A, 2014, 2, 20393–20401.
60. Pandey A, Singh G, Singh S, Jha K and Prakash C, J. Mech. Behav. Biomed. Mater, 2020, 108, 103781. [PubMed: 32469714]
61. Sabzi M, Babaahmadi M and Rahnama M, ACS Appl. Mater. Interfaces, 2017, 9, 24061–24070. [PubMed: 28640585]
62. Navarro-Baena I, Sessini V, Dominici F, Torre L, Kenny JM and Peponi L, Polym. Degrad. Stab, 2016, 132, 97–108.
63. Peponi L, Sessini V, Arrieta MP, Navarro-Baena I, Sonseca A, Dominici F, Gimenez E, Torre L, Tercjak A, López D and Kenny JM, Polym. Degrad. Stab, 2018, 151, 36–51.
64. Wang X, Yan H, Zhou Y, Lou X and Zhang Y, J. Control. Release, 2017, 259, e144–e145.
65. Wang X, Yan H, Shen Y, Tang H, Yi B, Qin C and Zhang Y, Tissue Eng. Part A, 2020, 27, 142–152. [PubMed: 32524903]
66. Samuel C, Barrau S, Lefebvre J-M, Raquez J-M and Dubois P, Macromolecules, 2014, 47, 6791–6803.
67. Amini M and Wu S, Comp. Comm, 2021, 23, 100564.
68. Wang S, Lu L, Gruetzmacher JA, Currier BL and Yaszemski MJ, Biomaterials, 2006, 27, 832–841. [PubMed: 16102819]
69. Nail LN, Zhang D, Reinhard JL and Grunlan MA, JoVE, 2015, e52981. [PubMed: 26556112]
70. Beltran FO, Houk CJ and Grunlan MA, ACS Biomater. Sci. Eng, 2021, 7, 1631–1639. [PubMed: 33667062]

71. Woodard LN, Kmetz KT, Roth AA, Page VM and Grunlan MA, Biomacromolecules, 2017, 18, 4075–4083. [PubMed: 29037044]
72. Zhang C, Cai D, Liao P, Su J-W, Deng H, Vardhanabhuti B, Ulery BD, Chen S-Y and Lin J, Acta Biomater, 2021, 122, 101–110. [PubMed: 33359298]
73. Antony GJM, Jarali CS, Aruna ST and Raja S, J. Mech. Behav. Biomed. Mater, 2017, 65, 857–865. [PubMed: 27810732]
74. Nöchel U, Reddy CS, Uttamchand NK, Kratz K, Behl M and Lendlein A, Eur. Polym. J, 2013, 49, 2457–2466.
75. Zhang X, Geven MA, Grijpma DW, Peijs T and Gautrot JE, Polymer, 2017, 122, 323–331.
76. Sharifi S, van Kooten TG, Kranenburg H-JC, Meij BP, Behl M, Lendlein A and Grijpma DW, Biomaterials, 2013, 34, 8105–8113. [PubMed: 23932501]
77. Boire TC, Gupta MK, Zachman AL, Lee SH, Balikov DA, Kim K, Bellan LM and Sung H-J, Acta Biomater, 2016, 34, 73–83. [PubMed: 27018333]
78. Xie Y, Lei D, Wang S, Liu Z, Sun L, Zhang J, Qing F-L, He C and You Z, ACS Biomater. Sci. Eng, 2019, 5, 1668–1676.
79. Le Fer G and Becker ML, ACS Appl. Mater. Interfaces, 2020, 12, 22444–22452. [PubMed: 32337967]
80. Yang L-Q, He B, Meng S, Zhang J-Z, Li M, Guo J, Guan Y-M, Li J-X and Gu Z-W, Polymer, 2013, 54, 2668–2675.
81. Baker RM, Henderson JH and Mather PT, J. Mater. Chem. B, 2013, 1, 4916–4920. [PubMed: 32261080]
82. Wang L, Shansky J, Borselli C, Mooney D and Vandenburgh H, Tissue Eng. Part A, 2012, 18, 2000–2007. [PubMed: 22646518]
83. Huang K, Yang M.-s., Tang Y.-j., Ling S-Y, Pan F, Liu X.-d. and Chen J, J. Biomater. Appl, 2020, 0885328220950062.
84. Zhang X, Liu K, Liu J, Ding Y, Li W and Zhang A, Eur. Polym. J, 2020, 141, 110092.
85. Touchet TJ and Cosgriff-Hernandez EM, in Advances in Polyurethane Biomaterials, eds. Cooper SL and Guan J, Woodhead Publishing, 2016, pp. 3–22.
86. Matsumoto H, Ishiguro T, Konosu Y, Minagawa M, Tanioka A, Richau K, Kratz K and Lendlein A, Eur. Polym. J, 2012, 48, 1866–1874.
87. Kai D, Prabhakaran MP, Chan BQY, Liow SS, Ramakrishna S, Xu F and Loh XJ, Biomed. Mater, 2016, 11, 015007. [PubMed: 26836757]
88. Song JJ, Chang HH and Naguib HE, Eur. Polym. J, 2015, 67, 186–198.
89. Gu S-Y, Liu L-L and Gao X-F, Polym. Int, 2015, 64, 1155–1162.
90. Shao L.-n., Dai J, Zhang Z.-x., Yang J.-h., Zhang N, Huang T and Wang Y, RSC Adv., 2015, 5, 101455–101465.
91. Yu J, Xia H, Teramoto A and Ni Q-Q, J. Biomed. Mater. Res. A, 2018, 106, 244–254. [PubMed: 28880433]
92. Yan B, Gu S and Zhang Y, Eur. Polym. J, 2013, 49, 366–378.
93. Sambasivam M, White R and Cutting K, in Wound Healing Biomaterials, ed. Ågren MS, Woodhead Publishing, 2016, pp. 251–260.
94. Ashida K and Iwasaki K, in Handbook of Plastic Foams, ed. Landrock AH, William Andrew Publishing, Park Ridge, NJ, 1995, pp. 11–220.
95. Singhal P, Rodriguez JN, Small W, Eagleston S, Van de Water J, Maitland DJ and Wilson TS, J. Polym. Sci., Part B: Polym. Phys, 2012, 50, 724–737.
96. Singhal P, Small W, Cosgriff-Hernandez E, Maitland DJ and Wilson TS, Acta Biomater, 2014, 10, 67–76. [PubMed: 24090987]
97. Hasan SM, Harmon G, Zhou F, Raymond JE, Gustafson TP, Wilson TS and Maitland DJ, Polym. Adv. Technol, 2016, 27, 195–203. [PubMed: 30034202]
98. Cai Y, Jiang J-S, Liu Z-W, Zeng Y and Zhang W-G, Compos. Part A Appl. Sci. Manuf, 2013, 53, 16–23.
99. Bothe M, Mya KY, Jie Lin EM, Yeo CC, Lu X, He C and Pretsch T, Soft Matter, 2012, 8, 965–972.

100. Montgomery M, Davenport Huyer L, Bannerman D, Mohammadi MH, Conant G and Radisic M, ACS Biomater. Sci. Eng, 2018, 4, 3691–3703. [PubMed: 33429599]
101. Liu Y, Fang N, Liu B, Song L, Wen B and Yang D, Mater. Lett, 2018, 233, 78–81.
102. Gao H-L, Lu Y, Mao L-B, An D, Xu L, Gu J-T, Long F and Yu S-H, Mater. Horiz, 2014, 1, 69–73.
103. Yan K, Xu F, Li S, Li Y, Chen Y and Wang D, Colloids Surf. B: Biointerfaces, 2020, 190, 110907. [PubMed: 32120129]
104. Lendlein A, Balk M, Tarazona NA and Gould OEC, Biomacromolecules, 2019, 20, 3627–3640. [PubMed: 31529957]
105. Wang J, Quach A, Brasch ME, Turner CE and Henderson JH, Biomaterials, 2017, 140, 150–161. [PubMed: 28649015]
106. Tseng L-F, Mather PT and Henderson JH, Acta Biomater, 2013, 9, 8790–8801. [PubMed: 23851156]
107. Yang P, Baker RM, Henderson JH and Mather PT, Soft Matter, 2013, 9, 4705–4714.
108. Safranski DL and Griffis JC, in Shape-Memory Polymer Device Design, eds. Safranski DL and Griffis JC, William Andrew Publishing, 2017, pp. 189–222.
109. Webber MJ, Khan OF, Sydlik SA, Tang BC and Langer R, Ann. Biomed. Eng, 2015, 43, 641–656. [PubMed: 25201605]
110. Belouin T, Journal, 2019, 84, 4821–4823.

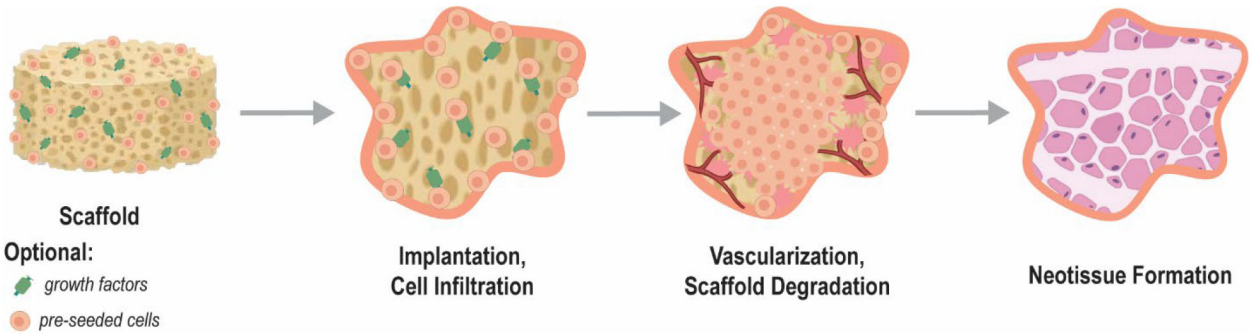

Figure 1.

Schematic showing the general stages of tissue engineering (TE) whereby a highly porous scaffold, optionally loaded with growth factors and/or pre-seeded with cells, promotes tissue healing. Eventually the scaffold construct degrades and is replaced with healthy neotissue.

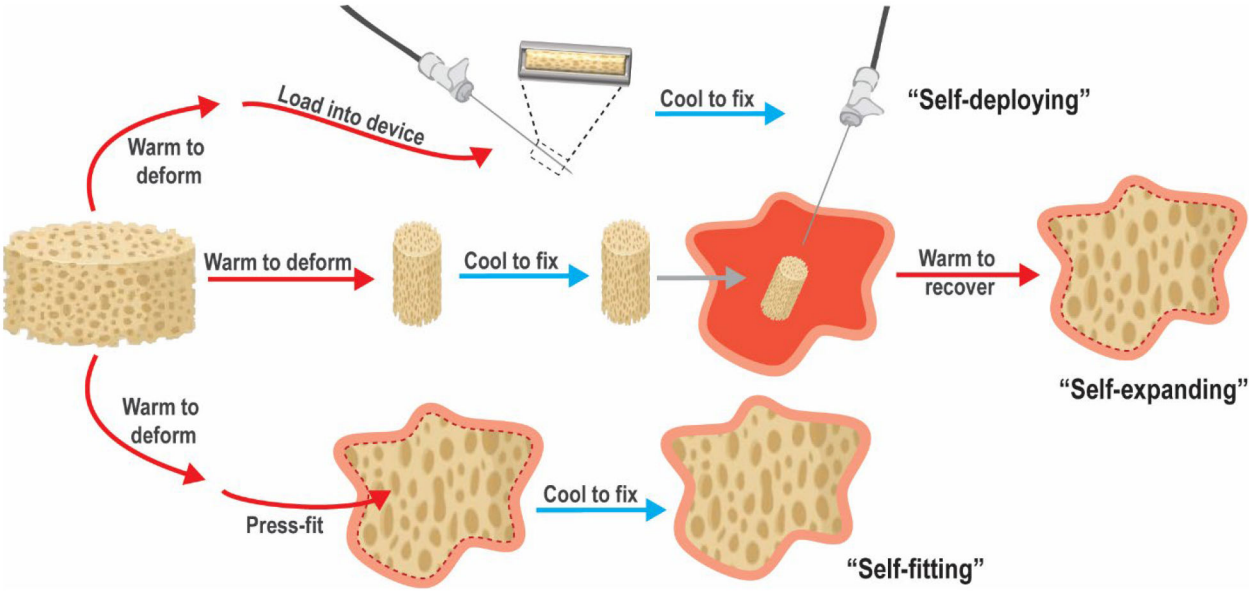

Figure 2.
Classes of SMP scaffolds based on mode of delivery into tissue defect.

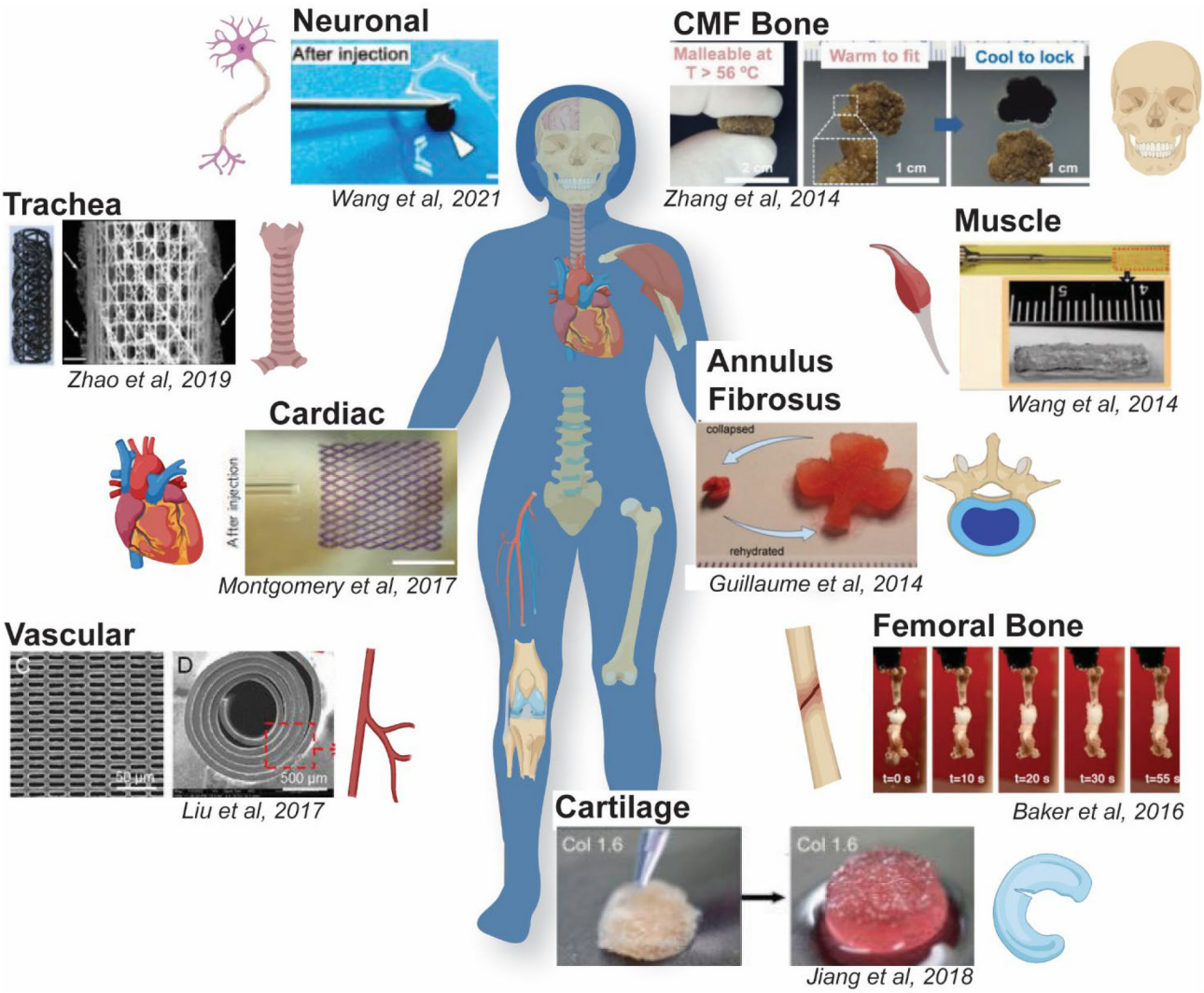

Figure 3.
Utility of smart SMP scaffolds in the regeneration of various tissues.

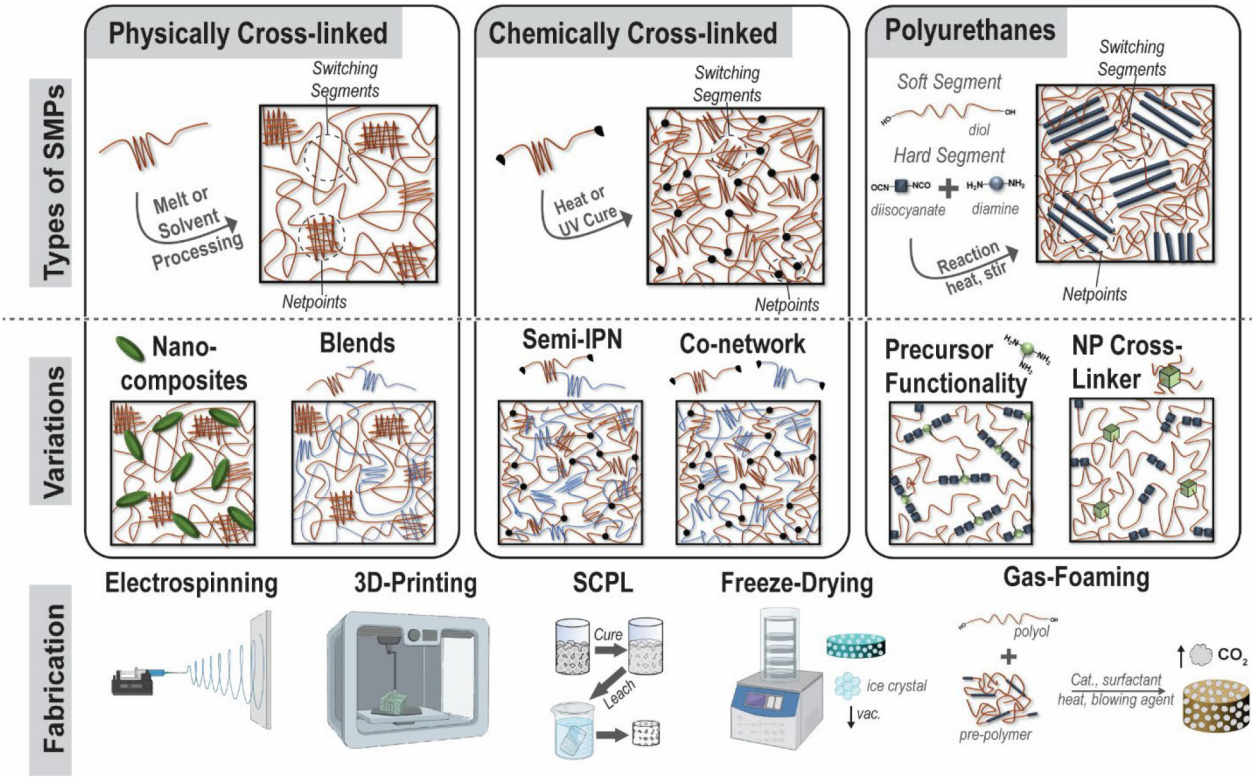

Figure 4.

(top) Classes of SMPs used to prepare smart scaffolds: physically cross-linked, chemically cross-linked, and PU systems. (middle) Variations to these main SMP classes that afford property tunability. (bottom) Different fabrication methods used to achieve smart scaffolds with targeted morphological features.

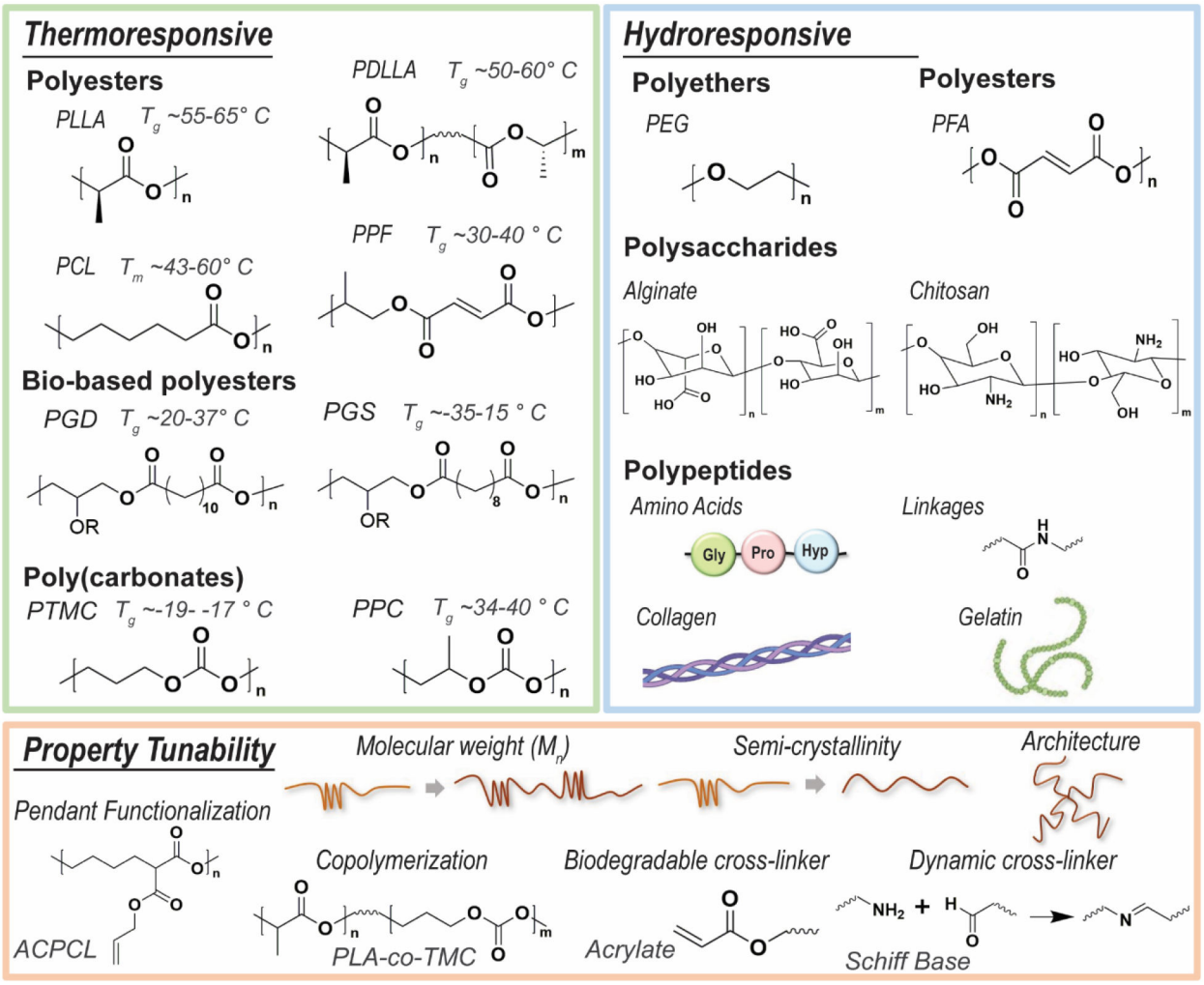

Figure 5.

SMPs typically used to achieve smart scaffolds with thermoresponsive and/or hydroresponsive behaviors, and additional ways that SMP scaffold properties may be tuned.

Table 1.

Select recent smart scaffolds for targeted tissue regeneration and their key properties.

Tissue	SMP Material	Additives	Intended Functionality	Transition Temperature (T_{trans})	Fabrication	Year	Ref
Bone	SMPU based on PCL or PLLA segments + PEG or gelatin	SPIO NPs	Self-expanding	Tuned to ~ T_{body} via plasticization	3D printing (i.e. FDM)	2018	35
	PCL/dextran carbodiimide linker	HAp coating	Self-expanding	Tuned to ~ T_{body} via PCL/dextran ratio	SCPL	2020	38
	PCL-DA	Polydopamine coating Cell adhesion peptide (RGD)	Self-fitting	$T_{m,PCL}$ ~ 55 °C	SCPL	2015	40
	tBA/BA tEG-DMA linker		Self-expanding	45 °C tuned via tBA/BA ratio	SCPL	2016	41
	SMPU based on PCL segments	HAp	Self-expanding	$T_{m,PCL}$ ~ 40 °C	Gas foaming	2018	42
Cartilage	Alginate carbodiimide linker	Type II collagen coating	Self-expanding	Hydroresponsive	Freeze drying	2017	43
	Collagen carbodiimide linker	Pre-seeded chondrocytes	Self-expanding	Hydroresponsive	Freeze drying	2018	44
	PGS/PPS	Kartogenin	Self-deploying	$T_{m,PGS}$ ~ 35–45 °C	SCPL	2020	45
	PLLA	Cartilaginous particles from iPS cells	Self-fitting	$T_{g,PLLA}$ ~ 60 °C	Threads woven into mesh tubes	2020	46
Cardiovascular	Soybean oil epoxidized acrylate		Self-expanding	T_{trans} ~ T_{body}	UV cure thin film + Stereolithography	2016	49
	Poly(octamethylene maleate (anhydride) citrate))	Rat or human CMs	Self-deploying	T_{trans} ~ T_{body}	Microfabrication	2017	50
	PEG-PCL-Ac		Self-deploying	T_{trans} ~ T_{body}	Melt cast + UV cure	2017	51
	PGD-Ac		Self-expanding	20–37 °C tuned via cure time	4D printing	2021	52
	PCL-*co*-ACPCL		Self-wrapping	T_{trans} ~ T_{body}	Laser ablation	2021	53
Skeletal Muscle	Alginate carbodiimide linker	Myoblasts, IGF-1 and VEGF	Self-deploying	Hydroresponsive	Freeze drying	2014	54
Neuronal	CNT-doped sericin	Pre-seeded BMSCs	Self-deploying	Hydroresponsive	Freeze drying	2021	55